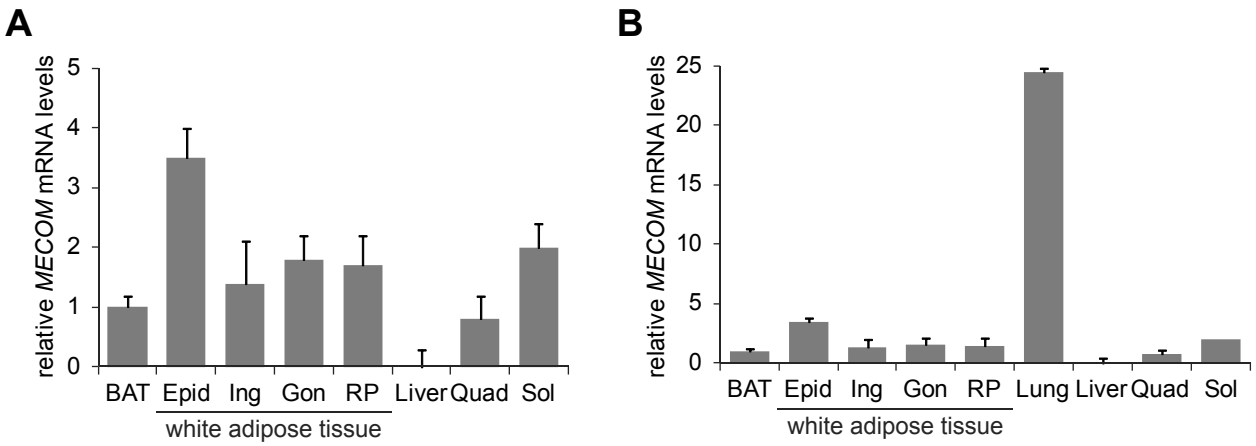

FIG. S1: *MECOM* is expressed in mouse fat depots. Real-time RT-PCR analysis of total RNA from a panel of mouse tissues. *MECOM* transcripts were found at moderate levels in all fat pads examined and in skeletal muscle; adult lung tissue has high expression and liver tissue has negligible expression. (A) and (B) are the same except for the expanded y-axis and addition of lung tissue in (B). BAT, brown adipose tissue; Epid, epididymal fat pad; Ing, inguinal fat pad; RP, retroperitoneal fat pad; Quad, quadriceps muscle; Sol, soleus muscle.

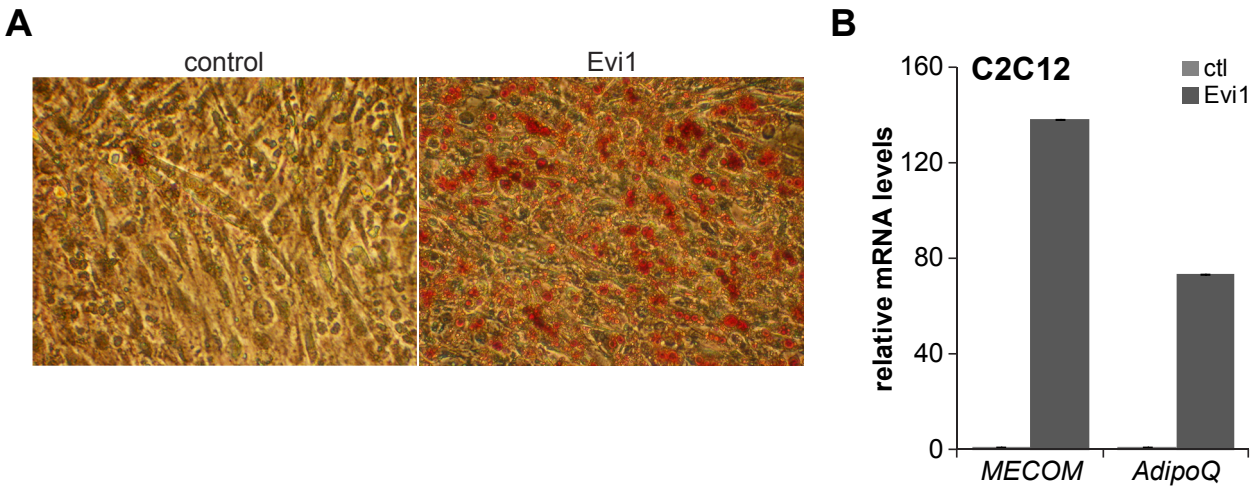

FIG. S2: Ectopic expression of Evi1 converts C2C12 myoblasts into adipocytes. C2C12 myoblasts were infected with retrovirus, vector (control) or Evi1, before being switched to adipocyte induction medium. (A) Oil Red O staining for lipid droplets. (B) Real-time PCR analysis showing overexpression of *Evi1* and activation of adipose marker *AdipoQ*.

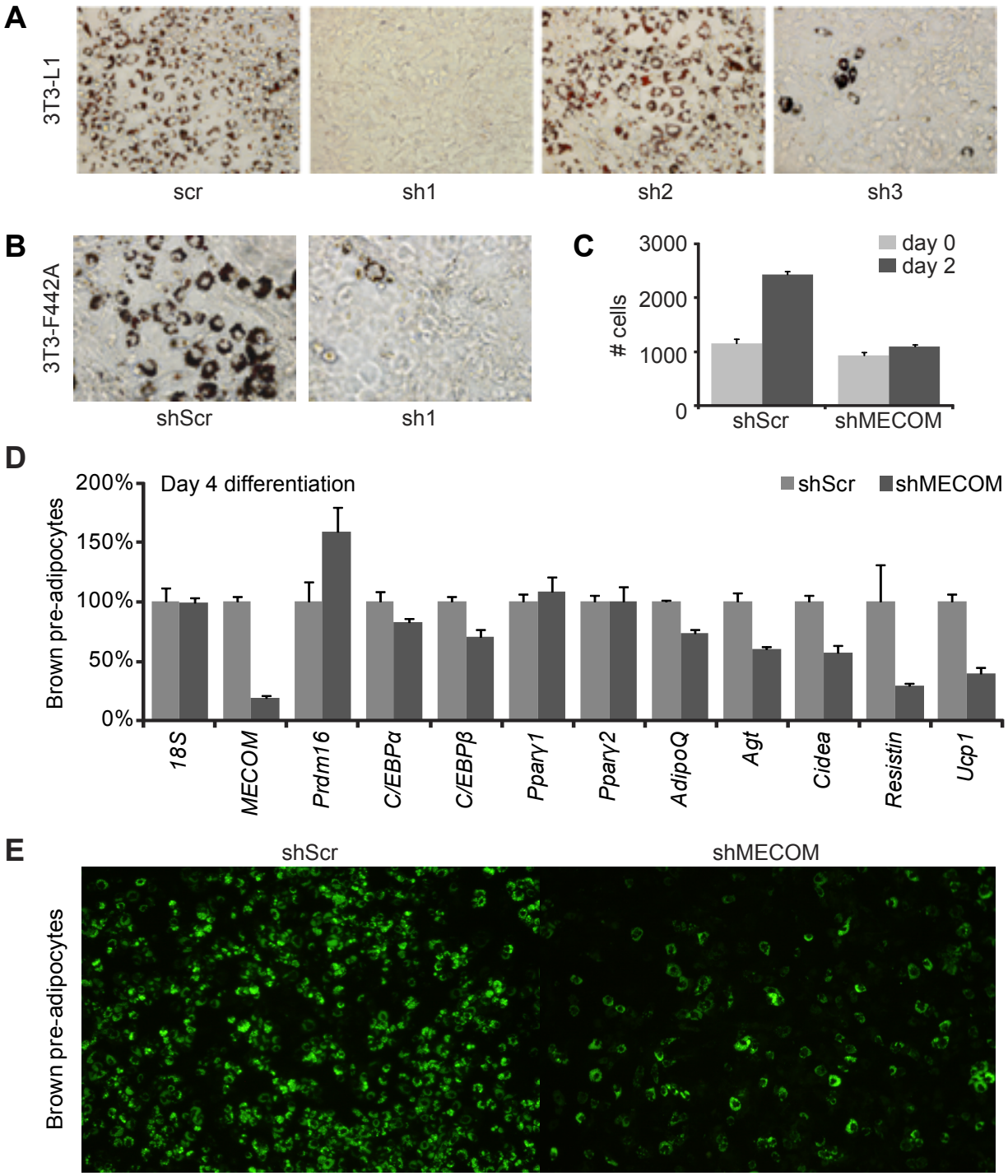

FIG. S3: shRNA knockdown of *MECOM* in pre-adipocytes inhibits adipogenesis. (A-B) Oil Red O staining of differentiating 3T3-L1 (A) and F442A (B) adipocytes demonstrates that shMECOM inhibits adipogenesis. Control shRNA (scr; scramble) or one of three shRNAs against *MECOM* (sh1, sh2, sh3). (C) Proliferation of 3T3-L1 cells after induction with differentiation medium. (D-E) Primary brown pre-adipocytes infected with shScr or shMECOM (sh1) and differentiated for 4 days. (D) Bodipy 493/503 staining for lipid accumulation. (E) RLT-PCR expression analysis.

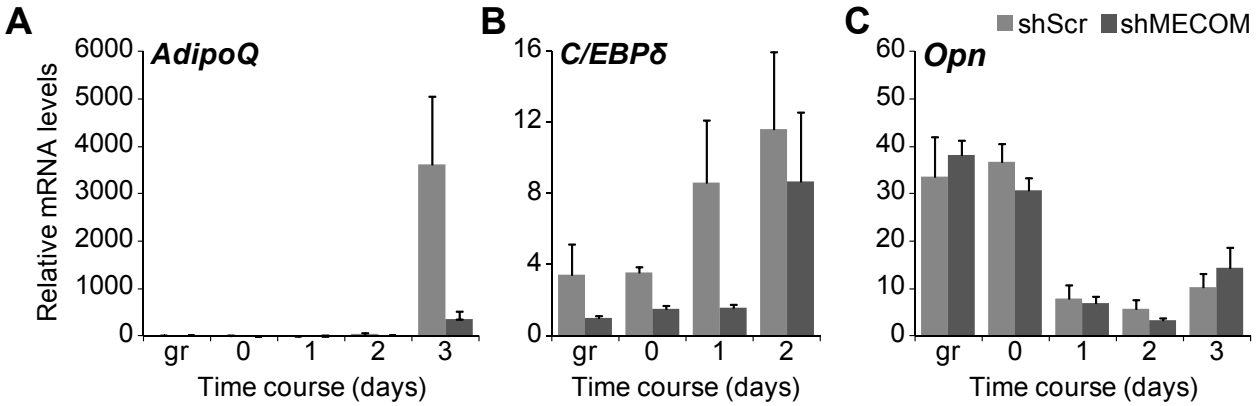

FIG. S4: shRNA knockdown of *MECOM* in 3T3-L1 cells inhibits adipogenesis but does not affect cell lineage determination. (A) Adipocyte differentiation marker *Adiponectin* (*AdipoQ*); (B) C/EBPδ; (C) osteogenesis marker *Osteopontin* (*Opn*); cartilage marker *collagen 2a* (*Col2a*) was undetected. Real-time PCR analysis of total RNA from 3T3-L1 infected with lentivirus expressing control (shScr) or *MECOM* (shMECOM) shRNAs. gr, sub-confluent growing conditions; 0 days, confluent cells at time of induction with differentiation medium; 1-3 days, time after addition of differentiation medium.

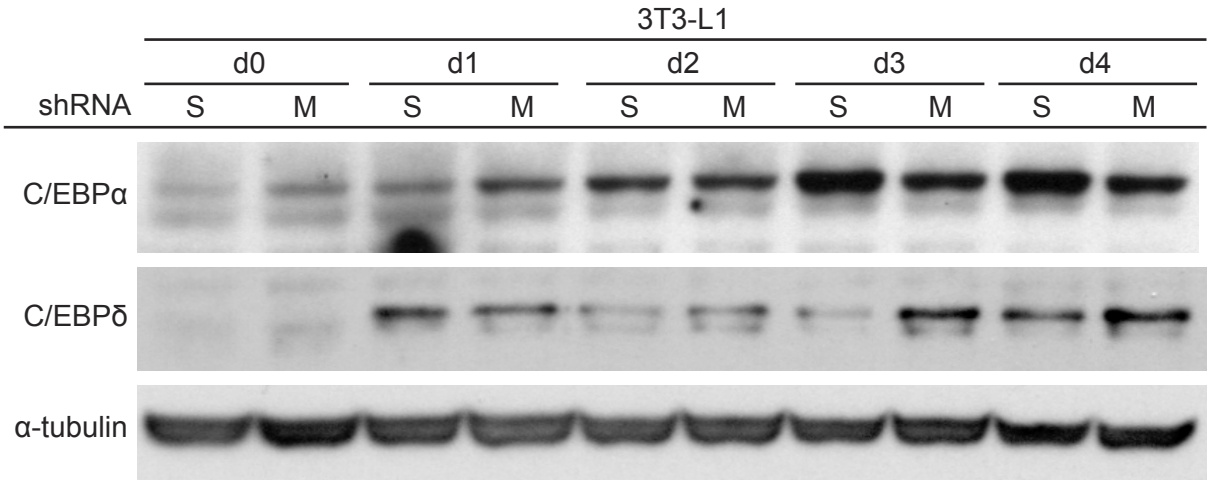

FIG. S5: Adipogenic transcription factor expression during differentiation in 3T3-L1 with shRNA knockdown of *MECOM*. Time points are prior to differentiation (d0) or days following induction (d1-d4), in cells infected with control (scramble, S) or MECOM (M) shRNAs.

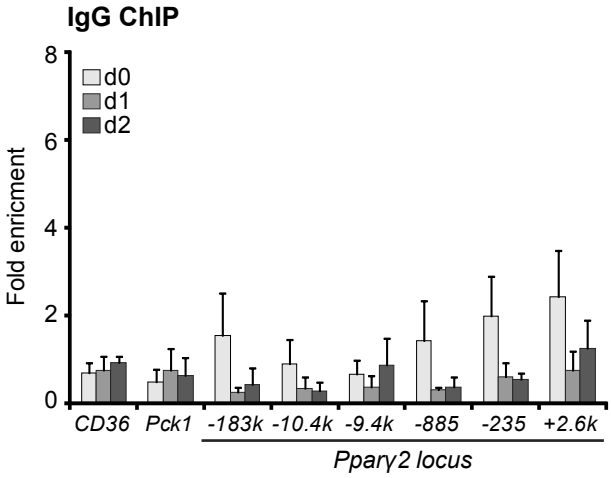

FIG. S6: Control IgG ChIP with does not enrich for C/EBPβ DNA binding sites at the *Pparγ2*- promoter. 3T3-L1 cells were harvested for ChIP at day-0 (blue), day-1 (red), or day-2 (green) of adipocyte differentiation. Chromatin enrichment was analysed by real-time PCR as %input recovery at non-target (*CD36; Pck1*) and *Pparγ2*-promoter sequences and normalized to *18S* %input to produce a fold-enrichment over background. *Pparγ2* locus primers are denoted (eg. +2.6k) in base-pairs relative to the *Pparγ2* transcriptional start site.

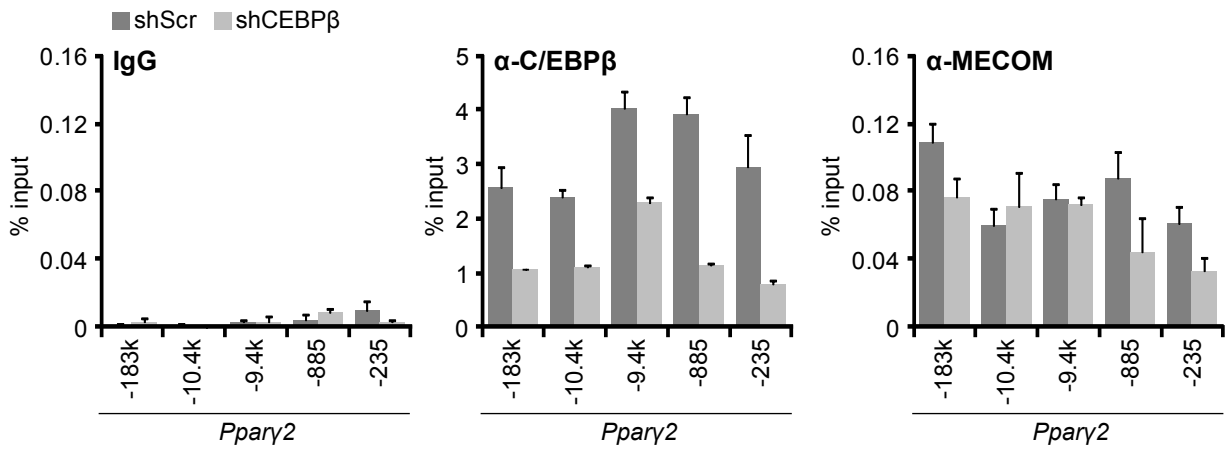

FIG. S7: Knockdown of C/EBPβ in 3T3-L1 reduces MECOM binding at *Pparγ2*. 3T3-L1 cells infected with shC/EBPβ and differentiated for one day for ChIP analysis. Chromatin enrichment was analysed by real-time PCR as %input. *Pparγ2* primers are denoted (eg. +2.6k) in base-pairs relative to the *Pparγ2* transcriptional start site.

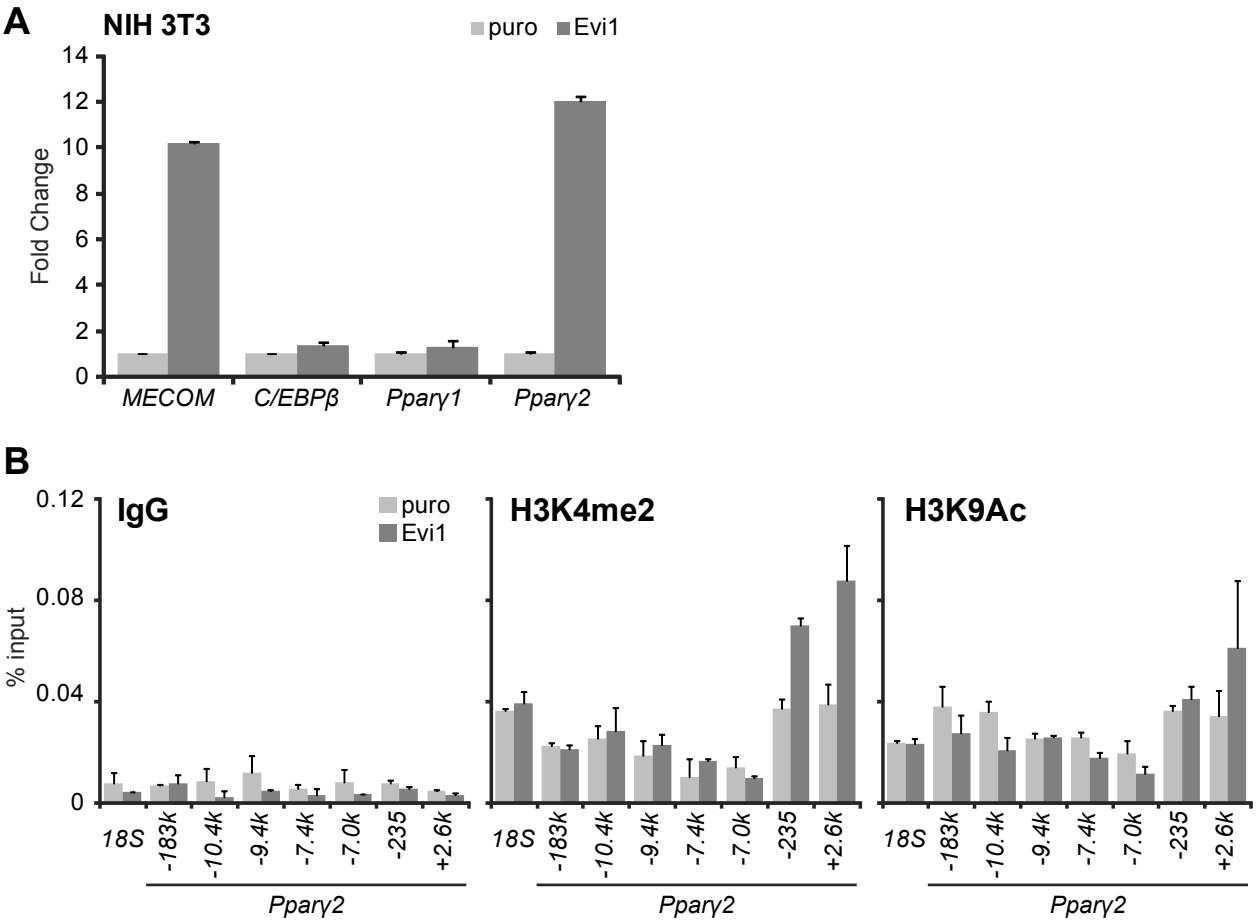

FIG. S8: Ectopic Evi1 expression in NIH 3T3 fibroblasts increases transcription-associated histone marks near the *Pparγ2* promoter. Evi1 was stably expressed in NIH 3T3 cells and grown to confluence (d0) prior to (A) expression analysis (normalized to *Tbp* and relative to puro) or (B) ChIP analysis for activating histone modifications. Chromatin enrichment was analysed by real-time PCR as %input recovery. *Pparγ2* locus primers are denoted (eg. +2.6k) in base-pairs relative to the *Pparγ2* transcriptional start site.

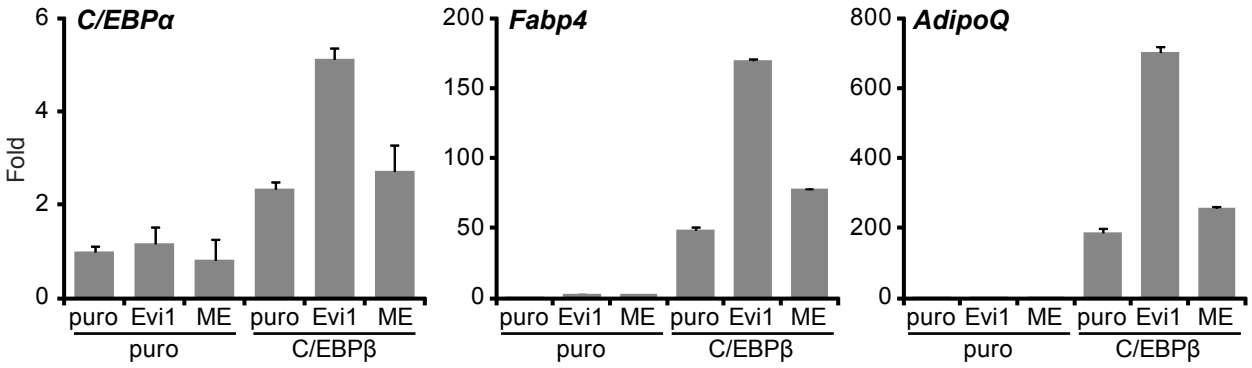

FIG. S9: Evi1 and C/EBPβ cooperate to convert NIH 3T3 cells into adipocytes. NIH 3T3 cells were stably infected with empty (puro), Evi1, or Mds1/Evi1 (ME) retrovirus, and re-infected with empty (puro) or C/EBPβ retrovirus. Gene expression was analysed at six days following addition of induction medium. Values normalized to *Tbp* expression and fold changes are expressed relative to the puro+puro controls.

Table S10 - Real-time PCR primers

Transcript	Forward		Reverse	
MECOM	5' atgcgtactttacagagatccg	3'	5' tccttgaagtgactgccattc	3'
Evi1	5' attgctgagttgaggccgta	3'	5' gggccctcttcactcttcat	3'
Mds1/Evi1	5' attccagctatggatgggaga	3'	5' ccagcttcctacatctggttg	3'
AdipoQ	5' gcactggcaagttctactgcaa	3'	5' gtaggtgaagagaacggccttgt	3'
C/EBPα	5' tgcgcaagagccgagataa	3'	5' cggtcattgtcactggtcaact	3'
C/EBPβ	5' acgacttcctctccgacctct	3'	5' cgaggctcacgtaaccgtagt	3'
Col2a	5' tcctctgcgatgacattatctg	3'	5' ttctcctttctgccccttg	3'
Fabp4	5' acaccgagatttccttcaaactg	3'	5' ccatctagggttatgatgctcttca	3'
Glut4	5' gtgactggaacactggtccta	3'	5' ccagccagttgcattgtag	3'
Lipe	5' gaacccctcatgtctcctct	3'	5' tgggagcaagaggtcttttag	3'
Opn	5' gtgatttgcttttgcctgtttg	3'	5' gagattctgcttctgagatggg	3'
Pparγ	5' gtgccagtttcgatccgtaga	3'	5' ggccagcatcgtgtagatga	3'
Pparγ1(1)	5' tgaaagaagcggtgaaccactg	3'	5' tggcatctctgtgtcaaccatg	3'
Pparγ1(2)	5' tgtgagaccaacagcctgac	3'	5' atatcagtggttcaccgcttc	3'
Pparγ2	5' tggcatctctgtgtcaaccatg	3'	5' gcatggtgccttcgctga	3'
Resistin	5' ttttcttccttgtccctgaactg	3'	5' gatcttcttgtcgatggcttcat	3'
Tbp	5' gaagctgcggtacaattccag	3'	5' ccccttgtacccttcaccaat	3'

Table S11 - ChIP PCR primers

Locus	Forward			Reverse		
18S	5'	agtccctgccctttgtacaca	3'	5'	cgatccgagggcctcact	3'
CD36-PPRE	5'	ccaacggaactgatttgagc	3'	5'	ttgctgctacactccagcat	3'
Pck1-PPRE	5'	gaactccgacaagcaagctc	3'	5'	tggcacttgagcaacaagac	3'
Pparg2-183k	5'	ctaggagctttgctggctaga	3'	5'	tgccaaacttcccaatgttat	3'
Pparg2-10.4k	5'	attgttttctccagctgccta	3'	5'	ttgaaatgagaagtgggaagg	3'
Pparg2-9.4k	5'	tcttcccagtaggaactgcat	3'	5'	ccttcatcatctcttctccaaa	3'
Pparg2-1.2k	5'	attgccaacttctcgattcac	3'	5'	tgataccccaaatggaataa	3'
Pparg2-885	5'	acttatgtgacaagggctgct	3'	5'	gcaaggaattgtggtcagttt	3'
Pparg2-235	5'	gaacagtgaatgtgtgggtca	3'	5'	ctgactgagagccagttgtga	3'
Pparg2+2.6k	5'	ctcaatatgcctcctcctctg	3'	5'	gctctattgcagcatttgtca	3'